

# Error Bounded Regular Algebraic Spline Curves \*

## (Extended Abstract)

Chandrajit L. Bajaj

Department of Computer Science,  
University of Texas, Austin, TX 78712  
Email: bajaj@cs.utexas.edu

Guoliang Xu †

State Key Laboratory of Scientific and  
Engineering Computing, ICMSEC,  
Chinese Academy of Sciences, Beijing

### 1 Introduction

We use segments of low degree algebraic curves  $G_{mn}(u, v) = 0$  in tensor product Bernstein-Bézier(BB) form defined within a parallelogram or rectangle, to construct  $G^1$  and  $G^2$  splines. A tensor product BB-form polynomial  $G_{mn}(u, v) = \sum_{i=0}^m \sum_{j=0}^n b_{ij} B_i^m(u) B_j^n(v)$  of bi-degree  $(m, n)$  has total degree  $m + n$ , however, the class of  $G_{mn}(u, v)$  is a subset of polynomials of total degree  $m + n$ .  $G^1$  (resp  $G^2$ ) continuity implies curve segments share the same tangent(curvature) at join points(knots). In each of the  $G^1$  and  $G^2$  constructions, we develop a spline curve family whose member satisfies given interpolation conditions. Each family depends on one free parameter that is related linearly to coefficients of  $G_{mn}(u, v)$ . Compared with A-spline segments defined in triangular (barycentric) BB-form [2], these algebraic curve segments in tensor product form have the following distinct features: (a) They are easy to construct. The coefficients of the bivariate polynomial that define the curve are explicitly given. (b) There exist convenient geometric control handles to locally modify the shape of the curve, essential for interactive curve design. (c) The spline curves, for the rectangle scheme, are  $\epsilon$ -error controllable where  $\epsilon$  is the pre-specified width of the rectangle. This feature is especially important for fitting to "noisy" data with uncertainty. (d) These splines curves have a minimal number of inflection points. Each curve segment of the spline curve has either no inflection points if the corresponding edge is convex, or one inflection point otherwise, and the join points of the curve segments are not inflection points. (e). Since the required bi-degree  $(m, n)$  for  $G^1$  and  $G^2$  is low(in this paper,  $\min\{m, n\} \leq 2$ ), the curve can be evaluated and displayed extremely fast. We explore both display via parameterization as well as recursive subdivision techniques(see [11]). (f) In the six spline families we discuss in sections 2 and 3, there are four cases with  $\min\{m, n\} = 1$ . In these cases, rational parametric expressions are easily derived. Hence, for

\*Supported in part by NSF grants CCR-9732306 and KDI-DMS-9873326

†Project 19671081 supported in part by NSFC. Currently visiting Center for Computational Visualization, UT, Austin, TX(<http://www.ticam.utexas.edu/CCV>).

Permission to make digital or hard copies of all or part of this work for personal or classroom use is granted without fee provided that copies are not made or distributed for profit or commercial advantage and that copies bear this notice and the full citation on the first page. To copy otherwise, to republish, to post on servers or to redistribute to lists, requires prior specific permission and/or a fee.

SCG'99 Miami Beach Florida

Copyright ACM 1999 1-58113-068-6/99/06...\$5.00

these cases, we have both the implicit form and the parametric form. Such dual form curves prove useful in several geometric design and computer graphics applications. (g) In treating a non-convex edge in the triangular scheme(see [2]), we need to break the edge into two parts by inserting an artificial inflection point. In the present parallelogram or rectangle scheme, we need not divide the edge, and the inflection point occurs only when necessitated by the end point interpolating conditions. These features make these error-bounded regular algebraic spline curves promising in applications such as interactive font design, image contouring etc.

Prior work on using implicit algebraic curve splines in data interpolation and fitting focus on using bivariate barycentric BB-form polynomials defined on plane triangles(see [1], [2], [4], [6], [7], [8], [10], [12], [13], [15]). To get a regular curve segment in a triangle, Sederberg, in [13], specified the coefficients of the BB-form of an implicitly defined bivariate polynomial in such a way that all the coefficients increase (or decrease) monotonically in the direction that is parallel to an edge of the triangle. In [12], Sederberg, Zhao and Zundel gave another similar set of conditions which guarantees the single sheeted property of their TPAC by requiring that  $b_{i0} \geq 0$ , that  $b_{0i}, b_{m-1,i} \leq 0$  and that the directional derivative of PAC(*piecewise algebraic curves*) with respect to any direction  $s = \alpha u$  be non-zero within the triangle domain, here  $b_{ij}$  denotes the Bézier coefficient. Related papers which construct families of  $G^1$  and  $G^2$  continuous cubic algebraic splines are given by Paluszny and Patterson [8, 9]. They use the following reduced form of the cubic  $F(s, t, u) = as^2u + bsu^2 - cst^2 - dt^2u + estu$ , with  $a > 0, b > 0, c > 0, d > 0$ , and  $(s, t, u)$  in BB-coordinates over a triangle and guarantee that the segment of the curve inside the triangle is convex. These results were further extended in [2] and [16]. Paper [2] provide formulation and construction of  $G^k$  A-spline defined in triangular BB-form. Paper [16] introduce the concept of a discriminating family of curves by which regular algebraic curve segments are isolated. Using different discriminating families, several characterizations of the BB-form of the implicitly defined real bivariate polynomials over the plane triangle and the parallelogram are given, so that the zero contours of the polynomials define smooth and single sheeted real algebraic (called regular) curve segments. In this extended abstract, we use two special families on rectangles and parallelograms, we call  $D_3$  and  $D_4$ -regular curves, respectively. Let  $[p_1p_2p_3p_4]$  be a parallelogram(or a rectangle) in the plane and consider the

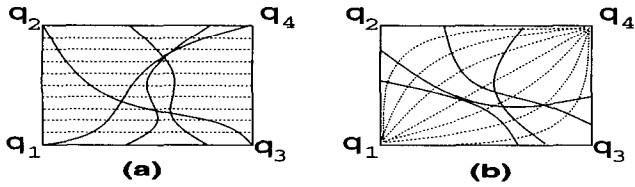


Figure 1.1: (a)  $D_3$  discriminating family (dotted line) and  $D_3$ -regular curves (real line). (b)  $D_4$  discriminating family (dotted line) and  $D_4$ -regular curves (real line).

discriminating families  $D_3$  (lines) and  $D_4$  (hyperbolic) below

$$D_3([p_1 p_2 p_3 p_4], [p_1 p_2], [p_3 p_4]) = \{v = s : s \in [0, 1]\},$$

$$D_4([p_1 p_2 p_3 p_4], p_1, p_4) = \{(1-s)u(1-v) - s(1-u)v = 0 : s \in [0, 1]\},$$

where  $p = (p_3 - p_1)u + (p_2 - p_1)v + p_1$ . The  $D_3$  (and  $D_4$ )-regular curves are smooth curve families that intersect with each member in the corresponding discriminating family only once, in the interior of the parallelogram (see Fig 1.1).

In this paper we have characterized the lowest bi-degree of tensor BB-form polynomial to achieve  $G^1$  and  $G^2$  continuous regular algebraic spline curves. Using the lowest bi-degree, we constructed explicit spline curve families whose members satisfied given  $G^1$  and  $G^2$  interpolation conditions. We also derived a geometric interpretation of each spline curve family, so that the shape of the individual curves can be controlled intuitively.

The rest of the extended abstract is as follows. In section 2 we show how a number of data fitting problem reduce to interpolating or approximating a polygonal chain of line segments with error bounds. In section 3, we discuss the problem of polygonal chain approximation by  $G^1$  and  $G^2$   $D_4$ -regular spline curves defined on parallelograms. In section 4, we discuss the problem of polygonal chain approximation by  $G^1$   $D_3$ -regular spline curves defined on rectangles. Examples are given in section 5. Section 6 concludes the paper.

## 2 Polygonal Chains

A polygonal chain is an ordered sequence of polygonal line segments, where any three adjacent points are not collinear. Several geometry processing tasks generate polygonal chains for shape representation in  $2D$ . Examples include shape or fonts design, fitting from “noisy” data, image contouring, snakes [5] and level set methods [14]. In this section, we mention a few of them that have some attached error or uncertainty.

**a. Noisy vertex data.** The vertex data (position) comes from a multi-sampling process with possible error. The error bound  $\epsilon$  is known in advance. Fig 2.1 show such a case. The white circles are repeatedly sampled points, the black dot are approximation of the sampled points. The approximation of the point can be computed as barycenters or centers of gravity or centers of bounding circular fits. The polygonal chain is obtained by connecting these black dots. Spline curve to be constructed interpolates the vertices of the polygonal chain. Hence the error around each vertex is bounded by  $\epsilon$ .

**b. Noisy curve data.** Suppose a curve is sampled with error bounded by  $\epsilon$  in sequence. The sampled point sequence

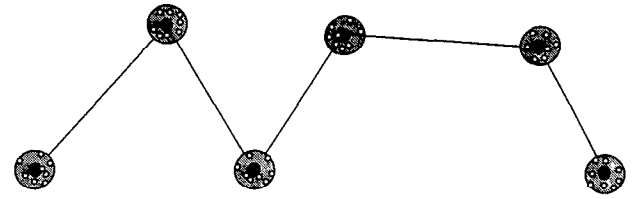


Figure 2.1: Polygonal chain extracted from over-sampled points.

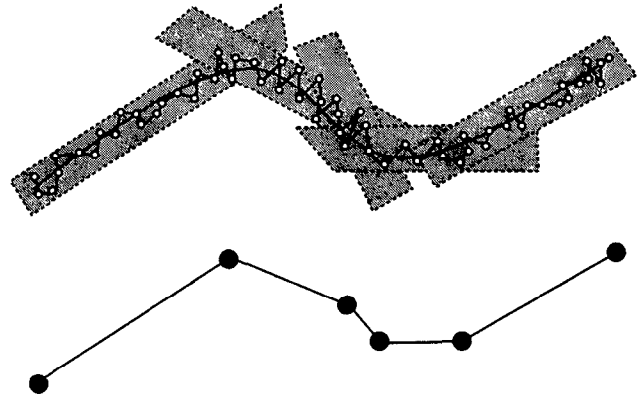


Figure 2.2: Polygonal chain from noisy curve data and using adaptive “strip pasting”: The white circles are original sampled points with error, and the black dots are the vertices of an extracted polygonal chain.

$\{v_i\}$  could be dense. To produce a polygonal chain to these points, we can use “strip pasting” technique. Choose the strip width to be no less than  $2\epsilon$ . Then use the minimal number strip to cover the samples points (see Fig 2.2). The vertices of the polygonal chain are the intersection points of two mid-axes of the adjacent strips. A computational method for obtaining the minimal number strips can be found in [3]. A greedy method to obtain the “strip pasting” uses an adaptive piecewise linear least square fitting, starting from one end of the data. The  $G^1$   $D_3$ -regular curves developed in section 4 is very suitable to interpolate these polygonal chains.

**c. Contour from an image.** An image could be treated as a piecewise  $C^0$  bi-linear function interpolating the intensity values at each pixel. A linear isocontour of the function is a polygonal chain. Of course, such a polygonal chain may be quite dense, hence a decimation step is often used to obtain coarser or multiresolution representations. Fig 2.3 shows an image and an isocontour with two decimated polygonal chains. The decimation method is established based on geometric error (Euclidean distance) control, that is, a point is removed if the distance of the point to the line, that interpolate its two neighbor points, is less than a given  $\epsilon$ . Hence all original points are within an  $\epsilon$ -neighborhood of the decimated polygonal chain. Again, the  $G^1$   $D_3$ -regular curves defined on rectangles with rectangle-width  $2\epsilon$  are just the right tools to provide smooth approximation of these polygonal chains. The two decimated polygonal chains in Fig 2.3 are obtained by taking  $\epsilon$  to be 0.05 and 0.25, respectively.

**d. Polygonal chain to polygonal chain.** One polygonal chain could be produced from another polygon chain by

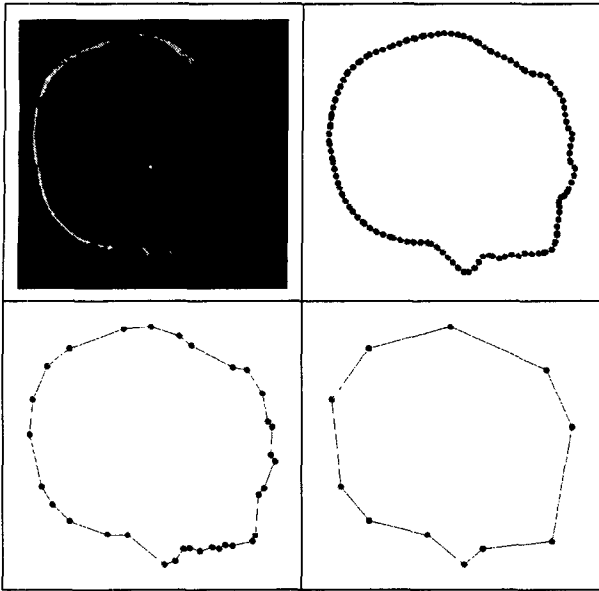


Figure 2.3: From an image to polygonal chains.

subdivision or corner cutting. Fig 2.4 shows three polygonal chains obtained by corner cutting with cutting ratios 0.25 and 0.5, respectively. When the cutting ratios is 0.5, then each edge of the new polygonal chain is *convex* (see the next section for the definition of a *convex* edge) if the tangents at the vertices are taken to be the original edges. This kind polygonal chain is suitable for triangular A-splines[2] as well as our  $D_3$ -regular curves (see section 3.1). The vertices of polygonal chain (d) are away from the original edge by a specified distance  $\delta$ . We call this as “offset corner cutting”. The offset will make constructed  $D_4$ -regular curves go around the original vertices. This is suitable to approximate over-sampled noisy vertex data as mentioned earlier.

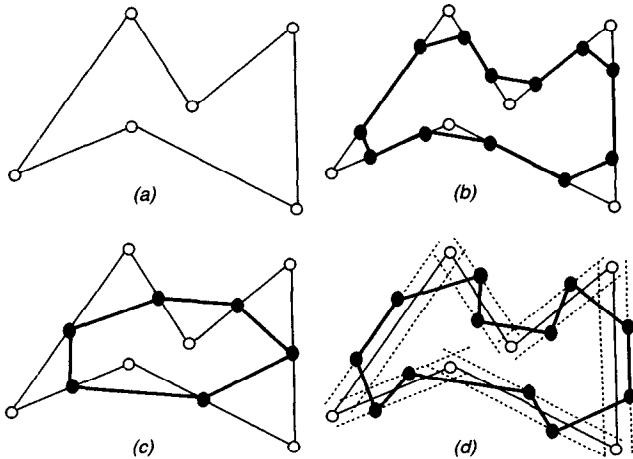


Figure 2.4: (a). An input polygonal chain; (b) Corner cut with cutting ratio 0.25; (c) Corner cut with cutting ratio 0.5 yielding a convex polygon; (d) Offset corner cut with cutting ratio 0.25.

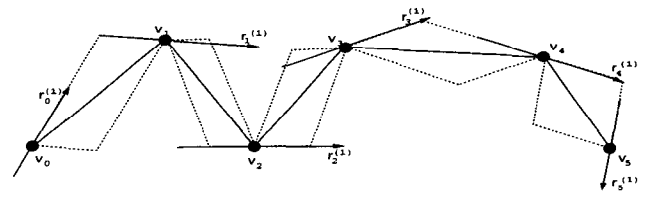


Figure 3.1: Parallelogram chain.

### 3 Polygonal Chain Approximation by $D_4$ -Regular Spline Curves

The regular spline curve consists of a chain of curve segments defined by the zero contour of a bivariate polynomial  $G_{mn}(u, v) = \sum_{i=0}^m \sum_{j=0}^n b_{ij} B_i^m(u) B_j^n(v)$  on a parallelogram  $[p_1 p_2 p_3 p_4]$ , where  $(u, v)^T \in [0, 1] \times [0, 1]$  relates to a point  $p = (x, y)^T \in [p_1 p_2 p_3 p_4]$  by the map

$$p = (p_3 - p_1)u + (p_2 - p_1)v + p_1, \quad (3.1)$$

where  $p_1, p_2, p_4, p_3$  are clockwise, any three of them are not collinear and  $p_1 + p_4 = p_2 + p_3$ .

Given an input polygonal chain, denoted by its vertices  $\{v_i\}_{i=0}^N$ , we use  $D_4$ -regular curves to smoothly approximate it, by interpolating the vertices with given first (for  $G^1$  continuity) and the second (for  $G^2$  continuity) order derivatives. These derivatives can be estimated from the given data by some known techniques, such as divided differences or local interpolation by parametric curve (see [2] for e.g.). Let the first order derivative  $r_i^{(1)}$  and the second order derivative  $r_i^{(2)}$  at  $v_i$  be given in the parametric form. Furthermore, without loss of generality, we assume that  $r_i^{(1)}$  and  $r_i^{(2)}$  are plane vectors and come from a parametric curve  $r(l)$  at  $l = l_i$ , where  $l$  is the arc length. Otherwise, we transform the derivatives by  $\tilde{r}_i^{(1)} = r_i^{(1)} / \|r_i^{(1)}\|$ ,  $\tilde{r}_i^{(2)} = r_i^{(2)} / \|r_i^{(1)}\|^2 - (r_i^{(1)T} r_i^{(2)}) r_i^{(1)} / \|r_i^{(1)}\|^4$  so that  $\tilde{r}_i^{(1)}$  and  $\tilde{r}_i^{(2)}$  have the required properties.

#### Step 1. Form a parallelogram chain

For each line segment (edge) of the polygonal chain, construct a parallelogram such that (see Fig 3.1, where the arrows are tangent vectors): (i) the line segment is one of the diagonals of the parallelogram; (ii) the tangent line of a vertex is contained in the two incident parallelograms.

In constructing parallelograms, we distinguish between *convex* and *non-convex* edges. For an edge  $[v_{i-1} v_i]$ , if the two tangent lines at  $v_{i-1}$  and  $v_i$  intersect at a point that lies in the region bounded by half-spaces  $(p - v_i)^T (v_i - v_{i-1}) \leq 0$  and  $(p - v_{i-1})^T (v_i - v_{i-1}) \geq 0$ , then the edge is called *convex*. Otherwise it is *non-convex*. In Fig 3.1,  $[v_0 v_1]$ ,  $[v_3 v_4]$  and  $[v_4 v_5]$  are convex edges,  $[v_1 v_2]$  and  $[v_2 v_3]$  are non-convex edges. For a convex edge, the corresponding parallelogram can be formed by the four points  $p_1, v_{i-1}, p_2, v_i$ , where  $p_1$  is the intersection point of the two tangents,  $p_2 = v_{i-1} + v_i - p_1$ . For a non-convex edge, take one point on each side of the edge such that  $p_2 + p_1 = v_{i-1} + v_i$ . These two points and the endpoints of the edge form the parallelogram.

#### Step 2. Construct $D_4$ -Regular Curves

For each parallelogram, construct a  $D_4$ -regular curve, such that it interpolates the endpoints of the line segment and has the given first order or second order derivatives. Let  $G_{mn}(u, v) = 0$  be the curve defined on  $[p_1 p_2 p_4 p_3]$ , where  $p_1$  and  $p_4$  are the interpolation points. Then by the map (3.1),

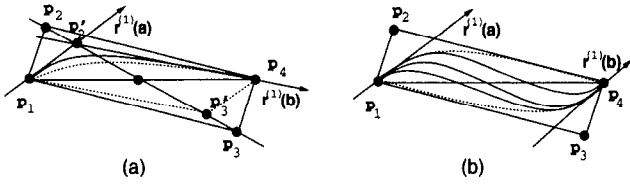


Figure 3.2: (a). Symmetric parallelogram about the tangent and the curve family for a convex edge; (b). The curve family for a non-convex edge

we have  $[u, v]^T = [p_3 - p_1, p_2 - p_1]^{-1}[p - p_1] = M[p - p_1]$ . Suppose the curve is parameterized as  $r(l)$  and let

$$r^{(k)}(l) = [p_3 - p_1, p_2 - p_1][\alpha_k(l), \beta_k(l)]^T = M^{-1}[\alpha_k(l), \beta_k(l)]^T. \quad (3.2)$$

That is,  $\alpha_k(l), \beta_k(l)$  are the decomposition coefficients of  $r^{(k)}(l)$  on  $p_3 - p_1$  and  $p_2 - p_1$ .

### 3.1 A $G^1$ Curve Spline Family

**A. Convex edge.** Let  $[p_1p_4]$  be a convex edge, and  $[p_1p_2p_3p_4]$  be the parallelogram. Assume  $p_1 = r(a)$ ,  $p_4 = r(b)$  for some  $a$  and  $b$  with  $a < b$ , and assume  $\beta_1(a) > \alpha_1(a)$ ,  $\beta_1(b) < \alpha_1(b)$ . Take  $m = n = 1$ .

#### 1. Construction Formulas.

$$b_{00} = b_{11} = 0, \quad b_{10} = 1, \quad b_{01} = \frac{1-\lambda}{\lambda} \in (-1, 0), \quad \lambda > 1, \quad (3.3)$$

$$p_2 = \lambda p'_2 + (1-\lambda)p'_3, \quad p_3 = (1-\lambda)p'_2 + \lambda p'_3, \quad (3.4)$$

where  $p'_2$  is the intersection point of the tangent lines of  $p_1$  and  $p_4$  (see Fig 3.2(a)),  $p'_3 = p_1 + p_4 - p'_2$  and  $\lambda$  is a free parameter. Note that the parallelogram  $[p_1p_2p_3p_4]$  varies with  $\lambda$ .

**2. Reformulation.** Let  $p = (p'_3 - p_1)s + (p'_2 - p_1)t + p_1$ . The curve  $G_{11}(u, v) = 0$  could be redefined on the smaller parallelogram  $[p_1p_2p'_3p_4]$  as:

$$B_\lambda : [4s - (s+t)^2]\lambda^2 - [4s - (s+t)^2]\lambda + s(1-t) = 0. \quad (3.5)$$

**3. Bounding Curves.** When  $\lambda = 1$ , the curve  $G_{11}(u, v) = 0$  degenerates to straight lines  $s = 0$  (the edge  $[p_1p'_2]$ ) and  $t = 1$  (the edge  $[p'_2p_4]$ ), while  $\lambda = \infty$ , the curve  $G_{11}(u, v) = 0$  degenerates to the curve  $B_\infty : 4s - (s+t)^2 = 0$ .

**4. Interpolation of an Interior Point.** For any given point  $p^* = (p'_3 - p_1)s^* + (p'_2 - p_1)t^* + p_1$  in the interior of the region  $\mathcal{E}_1$  enclosed by the curves  $B_1$  and  $B_\infty$ , there exists a unique  $\lambda \in (1, \infty)$ , that is

$$\lambda = \frac{1}{2} + \frac{t^* - s^*}{\sqrt{4s^* - (s^* + t^*)^2}}, \quad (3.6)$$

such that the curve  $G_{11}(u, v) = 0$  interpolates the point  $p^*$ .

**Theorem 3.1** For a convex edge, there exists a degree (1,1) ( $m = n = 1$ )  $D_4$ -regular curve family  $G_{11}(u, v) = 0$ , defined by (3.3)-(3.4), with a free parameter  $\lambda \in (1, \infty)$ , in the region  $\mathcal{E}_1$  enclosed by the curves  $B_1$  and  $B_\infty$ . Each curve in the family  $G^1$  interpolates the endpoints of the edge. For any given point  $p$  in the interior of  $\mathcal{E}_1$ , there exists a unique curve, defined by (3.3)-(3.4) and (3.6), in this family that interpolates the point  $p$ .

**Parameterization.** From  $G_{11}(u, v) = 0$ , we obtain the parameterized expression  $v = \frac{u}{u - b_{01}(1-u)}$ ,  $u \in [0, 1]$ .

**B. Non-convex edge.** We assume  $\beta_1(a) \geq \alpha_1(a)$ ,  $\beta_1(b) \geq \alpha_1(b)$ . Take  $m = 1, n = 2$ . If  $\beta_1(a) \leq \alpha_1(a)$ ,  $\beta_1(b) \leq \alpha_1(b)$ , take  $m = 2, n = 1$ .

#### 1. Construction Formulas.

$$b_{00} = b_{12} = 0, \quad b_{10} = 1, \quad b_{01} = -\frac{1}{2}\delta \leq 0, \quad b_{11} = -\frac{1}{2}\gamma b_{02} > 0, \quad (3.7)$$

where  $\delta = \frac{\alpha_1(a)}{\beta_1(a)}$ ,  $\gamma = \frac{\alpha_1(b)}{\beta_1(b)}$  and  $b_{02} < 0$  is a signed free parameter (see Fig 3.2(b) for the curve family).

#### 2. Bounding Curves.

$$L_0 : u(1-v) - \delta(1-u)v = 0, \quad L_{-\infty} : (1-u)v - \gamma u(1-v) = 0.$$

**3. Interpolation of an Interior Point.** For any given point  $p = (u, v)^T$  in the interior of the region  $\mathcal{E}_2$  enclosed by  $L_0$  and  $L_{-\infty}$ , take

$$b_{02} = -\frac{(1-v)[u(1-v) - \delta(1-u)v]}{v[(1-u)v - \gamma v(1-v)]}, \quad (3.8)$$

then the curve determined by  $b_{02}$  interpolates the point  $p$ .

**Theorem 3.2** For a non-convex edge, there exists a degree (1,2) (or (2,1))  $D_4$ -regular curve family, defined by (3.7) with a free parameter  $b_{02} \in (0, -\infty)$ , in the region  $\mathcal{E}_2$  enclosed by  $L_0$  and  $L_{-\infty}$ , whose members  $G^1$  interpolate the endpoints of the edge. For any given point  $p$  in  $\mathcal{E}_2$ , there exists a unique curve, defined by (3.7)-(3.8), in this family that interpolates the point  $p$ .

**Parameterization.** Since  $m = 1, n = 2$ , the curve can be expressed in rational parameterized form

$$u = -\frac{b_{01}B_1^2(v) + b_{02}B_2^2(v)}{B_0^2(v) + (b_{11} - b_{01})B_1^2(v) - b_{02}B_2^2(v)}, \quad v \in [0, 1].$$

**Shape Control Handles.** For the given polygonal chain, the shape control handles are: (i) the direction of tangent vector at each vertex; (ii) an interpolating point  $p$  in the region  $\mathcal{E}_1$ , for convex edges, or  $\mathcal{E}_2$ , for non-convex edges.

### 3.2 A $G^2$ Curve Spline Family

**A. Convex edge.** Let  $[p_1p_4]$  be a convex edge and  $[p_1p_2p_3p_4]$  be the parallelogram. Again, we assume  $\beta_1(a) > \alpha_1(a)$ ,  $\beta_1(b) < \alpha_1(b)$ . Furthermore, we assume that the parallelogram is constructed so that  $\alpha_1(a) = \beta_1(b) = 0$ . Now we need to take  $m = n = 2$ .

#### 1. Construction Formulas.

$$b_{00} = b_{01} = b_{12} = b_{22} = 0, \quad b_{02} = -1 \quad (3.9)$$

$$b_{10} = \frac{\beta_1(a)^2}{\alpha_2(a)} > 0, \quad b_{21} = -\frac{\alpha_1(b)^2}{\beta_2(b)} > 0, \quad 4b_{11} = 2b_{10} + 2b_{21} + 1 - b_{20}, \quad (3.10)$$

where  $b_{20}$  is a free parameter (see Fig 3.3(a) for the curve family).

**2. Interpolation of an Interior Point.** Parameter  $b_{20}$  can be used to interpolate one point  $(u, v)^T$  in the interior of the parallelogram with  $u < v$ . That is, take  $b_{20}$  to be

$$\frac{B_0^2(u)B_2^2(v) - b_{10}B_1^2(u)B_0^2(v) - [b_{21}B_2^2(u) + b_{11}B_1^2(u)]B_1^2(v)}{B_2^2(u)B_0^2(v)}. \quad (3.11)$$

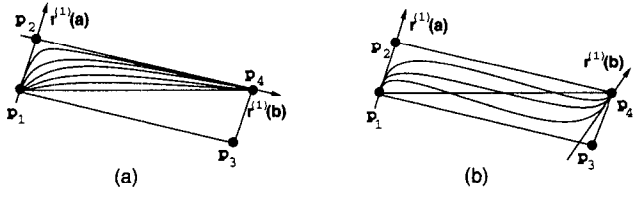


Figure 3.3: (a).  $G^2$  curve family for a convex edge; (b).  $G^2$  curve family for a non-convex edge.

3. *Reformulation.* Let  $\alpha_1 = 1 - v$ ,  $\alpha_2 = v - u$ ,  $\alpha_3 = u$ . Represent  $G_{22}(u, v)$  in the barycentric coordinate form  $\tilde{G}_{22}(\alpha_1, \alpha_2, \alpha_3)$  over the triangle  $[p_1 p_2 p_4]$ :

$$\tilde{G}_{22}(\alpha_1, \alpha_2, \alpha_3) := \sum_{i+j+k=3} a_{ijk} B_{ijk}^3(\alpha_1, \alpha_2, \alpha_3) \quad (3.12)$$

with

$$a_{300} = a_{210} = a_{003} = a_{012} = 0, \quad (3.13)$$

$$a_{111} = \frac{2b_{10} + 2b_{21} + b_{02} - b_{20}}{6}, \quad (3.14)$$

$$a_{201} = \frac{2}{3}b_{10}, \quad a_{102} = \frac{2}{3}b_{21}, \quad (3.15)$$

$$a_{120} = a_{021} = \frac{1}{3}b_{02}, \quad a_{030} = b_{02}. \quad (3.16)$$

**Theorem 3.3** For a convex edge, say  $[p_1 p_4]$ , there exists a degree (2,2) convex curve family in the triangle  $\mathcal{E}_3 = [p_1 p_2 p_4]$ , defined by (3.9)–(3.10), with  $b_{20}$  as a free parameter. Each member in the family  $G^2$  interpolates the endpoints of the edge. If  $b_{20} > 0$ , the curve is  $D_4$ -regular in the parallelogram  $[p_1 p_2 p_4 p_3]$ . If  $b_{20} \leq 0$ , the curve, that is re-defined by (3.12)–(3.16), is  $D_1$ -regular on the triangle  $[p_1 p_2 p_4]$ . For any given point  $p$  in the interior of  $\mathcal{E}_3$ , there exists a unique curve, defined by (3.9)–(3.11), in this family, that interpolates the point  $p$ .

**B. Non-convex edge.** Assume  $\beta_1(a) \geq \alpha_1(a)$ ,  $\beta_1(b) \geq \alpha_1(b)$  and the parallelogram is constructed so that  $\alpha_1(a) = 0$  or  $\alpha_1(b) = 0$ . Again, we take  $m = n = 2$ .

1. *Construction Formulas.*

$$b_{00} = b_{22} = 0, \quad b_{01} = -\delta b_{10}, \quad b_{21} = -\gamma b_{12}, \quad (3.17)$$

$$4b_{11} = 2(b_{12} + b_{01} + b_{10} + b_{21}) - (b_{02} + b_{20}), \quad (3.18)$$

$$b_{10} = \frac{1}{\Delta} \left\{ \alpha_1(a) [\beta_1(a) - \alpha_1(a)] [\gamma \beta_2(b) - \alpha_2(b)] + 2\alpha_1(a) \beta_1(a) [\beta_1(b) - \alpha_1(b)]^2 \right\} b_{20} - \frac{1}{\Delta} \left\{ \beta_1(a) [\beta_1(a) - \alpha_1(a)] [\gamma \beta_2(b) - \alpha_2(b)] \right\} b_{02}, \quad (3.19)$$

$$b_{12} = \frac{1}{\Delta} \left\{ \alpha_1(b) [\beta_1(b) - \alpha_1(b)] [\alpha_2(a) - \delta \beta_2(a)] + 2\alpha_1(b) \beta_1(b) [\beta_1(a) - \alpha_1(a)]^2 \right\} b_{02} - \frac{1}{\Delta} \left\{ \beta_1(b) [\beta_1(b) - \alpha_1(b)] [\alpha_2(a) - \delta \beta_2(a)] \right\} b_{20}. \quad (3.20)$$

where  $\delta = \frac{\alpha_1(a)}{\beta_1(a)}$ ,  $\gamma = \frac{\alpha_1(b)}{\beta_1(b)}$ ,  $\Delta = [\alpha_2(a) - \delta \beta_2(a)] [\gamma \beta_2(b) - \alpha_2(b)]$ ,  $b_{02} = -1$  and  $b_{20} > 0$  is a free parameter (see Fig 3.3(b) for the curve family).

2. *Bounding Curves.* Let  $G_{22}(u, v, b_{02}, b_{20})$  be defined by (3.17)–(3.20). Then the bounding curves are  $G_{22}(u, v, 1, 0) = 0$ ,  $G_{22}(u, v, 0, 1) = 0$ .

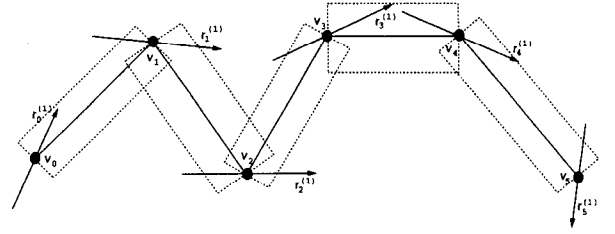


Figure 4.1: Rectangular chain.

**Theorem 3.4** For a non-convex edge, we have a one parameter  $D_4$ -regular curve family  $\{b_{20} G_{22}(u, v, 0, 1) - G_{22}(u, v, 1, 0) = 0 : b_{20} > 0\}$  whose members  $G^2$  interpolate the edge and have only one inflection point. For any given point  $p = (u^*, v^*)^T$  in the interior of the region  $\mathcal{E}_4$  enclosed by the curves  $G_{22}(u, v, 0, 1) = 0$  and  $G_{22}(u, v, 1, 0) = 0$  in the parallelogram, there exists unique curve in the family with  $b_{20} = G_{22}(u^*, v^*, 1, 0) / G_{22}(u^*, v^*, 0, 1)$  that interpolates the point  $p$ .

**Curve Evaluation and Display.** Since  $G_{22}(u, v)$  could be expressed as  $\sum_{i=0}^2 B_i(v) B_i^2(u)$  with  $B_0(v) < 0$ ,  $B_2(v) > 0$  on  $(0, 1)$ , the curve  $G_{22}(u, v) = 0$  can be evaluated for each  $v$  in  $(0, 1)$  by finding the zeros of a quadratic polynomial,  $B_i(v) = \sum_{j=0}^2 b_{ij} B_j^2(v)$ . For the case of a convex edge, it is possible that the quadratic has two zeros in  $(0, 1)$ , and the correct one is such that  $u < v$ . For the non-convex edge, the quadratic has exactly one zero in  $(0, 1)$ .

**Shape Control Handles.** For the given polygonal chain, the shape control handles of the curve are: (i) the direction of tangent vector at each vertex; (ii) the magnitude of the second order derivative vector (related to curvature) at each vertex; (iii) an interpolating point in the region  $\mathcal{E}_3$  for convex edges, or  $\mathcal{E}_4$  for non-convex edges.

## 4 Polygonal Chain Approximation by $D_3$ -Regular Curves

### Step 1. Form a Rectangular Chain

For each line segment(edge) of the polygonal chain, construct a rectangle such that (see Fig 4.1, where the arrows are tangent vectors) the line segment is in the middle of the rectangle. That is, two edges are parallel to the line segment at an equal distance  $\epsilon$  from it, and the other two edges are orthogonal to the line segment and pass through the endpoints of the line segment.

### Step 2. Construct the $D_3$ -regular Curves

For each rectangle, construct a  $D_3$ -regular curve, such that it interpolates the endpoints of the line segment and has given first order derivatives. Let  $[p_1 p_2 p_3 p_4]$  be a given rectangle,  $v_0 = (p_1 + p_2)/2$ ,  $v_1 = (p_3 + p_4)/2$  be the interpolation points and  $r_0^{(1)}$ ,  $r_1^{(1)}$  be the tangent vectors. Let  $G_{m1}(u, v) = \sum_{i=0}^m \sum_{j=0}^1 b_{ij} B_i^m(u) B_j^1(v)$ .

### 4.1 A $G^1$ Curve Spline Family

**A. Convex edge.** Suppose  $[v_0 v_1]$  be a convex edge. As (3.2), let  $r^{(1)} = \alpha_1(p_3 - p_1) + \beta_1(p_2 - p_1)$ . From the construction of the rectangular chain, we have  $\alpha_1(a) > 0$ ,  $\alpha_1(b) > 0$ . Now assume  $\beta_1(a) > 0$ ,  $\beta_1(b) < 0$  (the case  $\beta_1(a) < 0$ ,  $\beta_1(b) > 0$  is similar) and take  $m = 2$ ,  $n = 1$ .

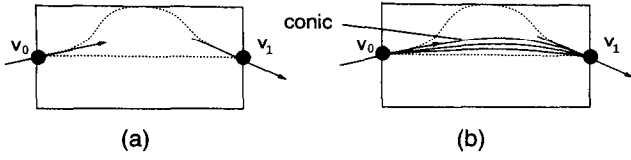


Figure 4.2: (a). Non-convex curve; (b). Convex curves.

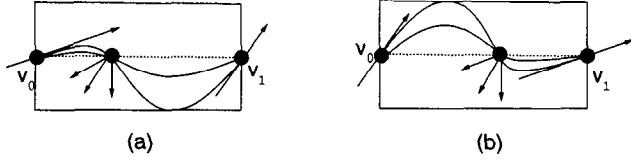


Figure 4.3: (a) The case  $\alpha \leq \beta$ ; (b) The case  $\alpha > \beta$ .

1. Construction Formulas.

$$\begin{aligned} b_{00} &= 1, \quad b_{21} = -b_{20}, \quad b_{01} = -1, \\ b_{10} + b_{11} &= 2\alpha = -2\beta b_{20}, \quad b_{20} = -\alpha\beta^{-1} > 0, \end{aligned} \quad (4.1)$$

where  $\alpha = \frac{\beta_1(a)}{\alpha_1(a)}$ ,  $\beta = \frac{\beta_1(b)}{\alpha_1(b)}$ ,  $b_{11}$  as a free parameter (see Fig 4.2(b) for the curve family).

2. Limitations on Free Parameters. To make the curves  $D_3$ -regular and convex, we enforce

$$b_{11} < b_{11}^* := \min \left\{ \sqrt{-\alpha\beta^{-1}}, \quad -\frac{1}{2} + \alpha [1 + \beta^{-1}] \right\}. \quad (4.2)$$

**Theorem 4.1** For a convex edge, let  $G_{21}(u, v, b_{11})$  be defined by (4.1), then we have a convex  $D_3$ -regular curve family  $\{G_{21}(u, v, b_{11}) = 0 : b_{11} < b_{11}^*\}$ , whose members  $G^1$  interpolate the endpoints of the edge. For any given point  $p = (u^*, v^*)^T$  in the region  $\mathcal{E}_5$  enclosed by the curve  $G_{21}(u, v, b_{11}^*) = 0$  and the line  $v = \frac{1}{2}$  there exists a unique  $b_{11}$  satisfying  $G_{21}(u^*, v^*, b_{11}) = 0$  such that the curve  $G_{21}(u, v, b_{11}) = 0$  interpolates the point  $p$ .

**B. Non-convex edge.** Assume  $\beta_1(a) \geq 0$ ,  $\beta_1(b) \geq 0$ . Take  $m = 3, n = 1$ .

1. Construction Formulas.

$$b_{00} = b_{30} = 1, \quad b_{01} = b_{31} = -1, \quad (4.3)$$

$$b_{10} + b_{11} = \frac{4}{3}\alpha, \quad b_{20} + b_{21} = -\frac{4}{3}\beta, \quad (4.4)$$

$$b_{11} + b_{20} = b_{10} + b_{21}, \quad (4.5)$$

$$b_{10} = b_{20} + \frac{2}{3}(\alpha + \beta), \quad b_{21} = b_{11} - \frac{2}{3}(\alpha + \beta), \quad (4.6)$$

where  $\alpha = \frac{\beta_1(a)}{\alpha_1(a)}$ ,  $\beta = \frac{\beta_1(b)}{\alpha_1(b)}$ ,  $b_{20}$  or  $b_{11}$  is a free parameter (see Fig 4.3 for the curve family).

2. Limitations on Free Parameters. To ensure the curves are  $D_3$ -regular and have only one inflection point, we require

$$b_{20} > \max \left\{ b_{20}^*, \frac{\alpha - \beta - 2\alpha\beta}{3\alpha}, \frac{\beta - \alpha - 2\beta^2}{3\beta} \right\}, \quad (4.7)$$

when  $\alpha \leq \beta$ ,

$$b_{11} < \min \left\{ b_{11}^*, \frac{\beta - \alpha + 2\alpha^2}{3\alpha}, \frac{\alpha - \beta + 2\alpha\beta}{3\beta} \right\}, \quad (4.8)$$

when  $\alpha > \beta$ , where  $b_{20}^*$  is the largest negative root of  $h(b_{20}) = 0$ ,  $b_{11}^*$  is the smallest positive root of  $g(b_{11}) = 0$  with

$$h(b_{20}) := 1 + 4b_{10}^3 + 4b_{20}^3 - 3b_{10}^2b_{20}^2 - 6b_{10}b_{20},$$

$$g(b_{11}) := 1 - 4b_{11}^3 - 4b_{21}^3 - 3b_{11}^2b_{21}^2 - 6b_{11}b_{21}.$$

3. Interpolation to a Normal. It should be noted that all the curves pass through the same point  $(u^*, \frac{1}{2})^T$  with  $u^* = \frac{\alpha}{\alpha + \beta}$  (see Fig 4.3). Since

$$\nabla G_{31}(u^*, \frac{1}{2}) = \left[ -\frac{2\alpha\beta}{\alpha + \beta}, -\frac{2(\alpha^3 + \beta^3)}{(\alpha + \beta)^3} - \frac{(6b_{20} + 4\beta)\alpha\beta}{(\alpha + \beta)^2} \right]^T,$$

by assigning a normal at  $(u^*, \frac{1}{2})^T$ , the unique  $b_{20}$  is determined.

**Theorem 4.2** For a non-convex edge, there exists a  $D_3$ -regular curve family  $\{G_{31}(u, v) = 0\}$  that has the following properties: (i). Each curve in the family  $G^1$  interpolates the edge. (ii). Each curve passes through the point  $(u^*, \frac{1}{2})^T$ . (iii). There is only one curve in that family that has the given normal at  $(u^*, \frac{1}{2})^T$ . (iv). The curve  $v = \frac{1}{2}$  and the curve given by  $b_{20} = b_{20}^*$  (if  $\alpha \leq \beta$ ) or  $b_{11} = b_{11}^*$  (if  $\alpha > \beta$ ) are the two limit curves of the family.

**Parameterization.** Since the curve is defined by  $G_{m1}(u, v) = \sum_{i=0}^m b_{i0}B_i^m(u) + v \sum_{i=0}^m (b_{i0} - b_{i1})B_i^m(u) = 0$ , it follows from (3.1) that

$$p = (p_3 - p_1)u - (p_2 - p_1) \frac{\sum_{i=0}^m b_{i0}B_i^m(u)}{\sum_{i=0}^m (b_{i0} - b_{i1})B_i^m(u)} + p_1,$$

for  $u \in [0, 1]$ .

**Shape Control Handles.** For the given polygonal chain, the shape control handles of the curve are: (i) the direction of the tangent vector at each vertex; (ii) an interpolating point in the region  $\mathcal{E}_5$ , for convex edges, or a normal at  $(u^*, \frac{1}{2})^T$ , for non-convex edges.

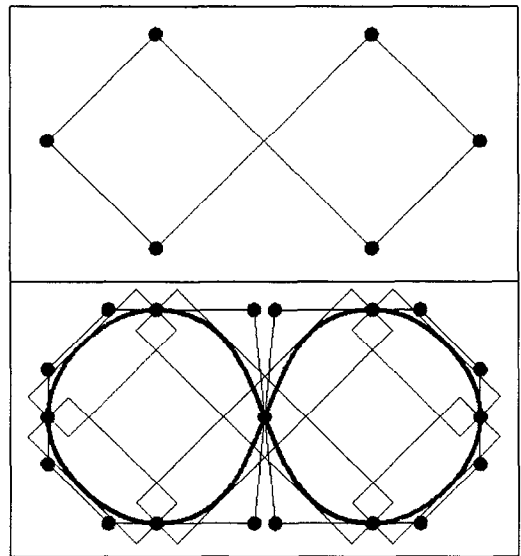


Figure 4.4: The top figure shows the input polygon. The bottom shows the  $G^1 D_4$ -regular curves and Bézier points interpolating the vertices of the polygon within prescribed bounds.

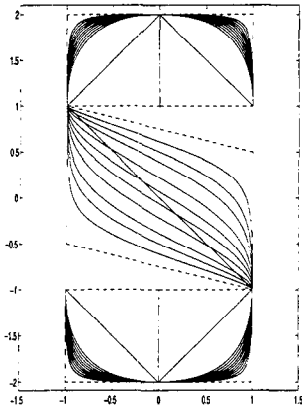


Figure 5.1:  $G^1$  families on parallelograms.

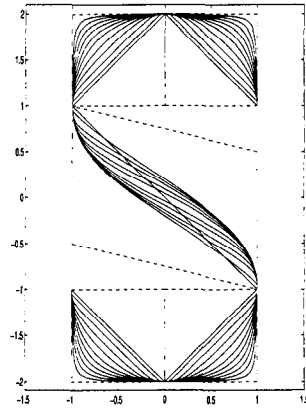


Figure 5.2:  $G^2$  families on parallelograms.

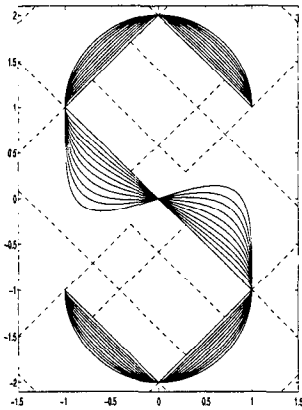


Figure 5.3:  $G^1$  families on rectangles with  $\epsilon = 1.0$ . The width of the rectangle is  $2\epsilon$ .

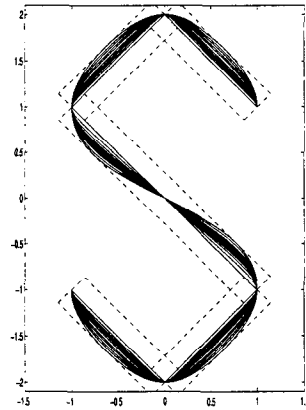


Figure 5.4:  $G^1$  families on rectangles with  $\epsilon = 0.2$ . The width of the rectangle is  $2\epsilon$ .

**Note.** In the six spline families we discuss in sections 3 and 4, there are four cases with  $\min\{m, n\} = 1$ . In these cases, rational parametric expressions are easily derived. Hence, for these cases, we have both the implicit form and the parametric form. For example, the  $G^1 D_3$ -regular curve could be transformed into parametric rational Bézier curve of degree 4. The bottom figure of Fig 4.4 shows the Bézier points of  $G^1 D_3$ -regular curve as well as the rectangle chain for the input polygonal chain (top figure). It is clear that the rectangles more tightly enclose the curve than the convex hull of the Bézier points. Furthermore, the shape of curve is easier to control using its implicit form than using its parametric form, since the implicit form has one free parameter while the rational Bézier of degree 4 has many more degrees of freedom. Also, the parameter change of the rational Bézier form may lead the curve out of the  $G^1 D_3$ -regular curve family.

## 5 Examples

To illustrate the data fitting flexibility of the spline curves introduced in the last two sections, we provide several examples. In all the examples, the input data are normalized into the cube  $[-5, 5] \times [-5, 5] \times [-5, 5]$ . In order to illustrate

the features for each case, we use the following regular data:

$$\begin{aligned} \{v_i\} &= \{(1, 1), (0, 2), (-1, 1), (1, -1), (0, -2), (-1, -1)\}, \\ \{r_i^{(1)}\} &= \{(0, 1), (-1, 0), (0, -1), (0, -1), (-1, 0), (0, 1)\}, \\ \{r_i^{(2)}\} &= \{(-1, 0), (0, -1), (1, 0), (-1, 0), (-1, 0), (1, 0)\}. \end{aligned}$$

In each case, ten curves are plotted (see Fig 5.1–5.4) for ten different parameters to show the curve family. The features of the curves shown in the figures coincide with the analysis in section 2 and 3.

For the convex edge, the  $G^1$  curves (in Fig 5.1) within a parallelogram are located away from the convex edge. In contrast, the  $G^1$  curves (Fig 5.3, 5.4) within a rectangle are located near the convex edge. The  $G^2$  curve family within a parallelogram (Fig 5.2) has both these features.

For the non-convex edge, the  $G^1$  curves (in Fig 5.1) within a parallelogram tend to go directly from one vertex to the other. Hence the curves have sharp changes in the tangent direction at the end points for the parameters near the boundary of its domain, even though the curves are rather straight in the middle. The  $G^2$  curves within a parallelogram (Fig 5.2) do not have sharp changes in the tangent direction. The  $G^1$  curves (Fig 5.3, 5.4) within a rectangle closely follow the letter S, and additionally, all pass through the same point. The curves in Fig 5.4 are  $G^1$  within the rectangle, but within a smaller size (width =  $2\epsilon$ , and  $\epsilon = 0.2$ , in contrast with  $\epsilon = 1.0$  in Fig 5.3) of rectangle. As one can observe, these curves shrink towards the edges of the shrunken rectangle.

In summary,  $D_3$ -regular and  $D_4$ -regular curves have several common features and have different features as well. For example, both of them can be sharp (rapid change of tangent line) at the vertices. However,  $D_4$ -regular curves can also be very flat (slow change of tangent line) around vertices and sharp at other parts.  $D_3$ -regular curves cannot be very flat around vertices if  $\epsilon$  is small. These features can be utilized in shape design where sharp and flat features are required.

The features of the curves introduced in this paper strongly suggest that these tensor-product BB-form curve families serve a variety of geometric design and computer graphics applications. Fig 5.5 and 5.6 show some fitting examples from real data. The polygonal chains in Fig 5.5 (left) are decimated contours stack of a human femur. Fig 5.5 (right) are the results of  $G^1 D_4$ -regular curve approximation. The polygonal chains in Fig 5.6 are the decimated results of the polygonal chain shown in Fig 2.3.

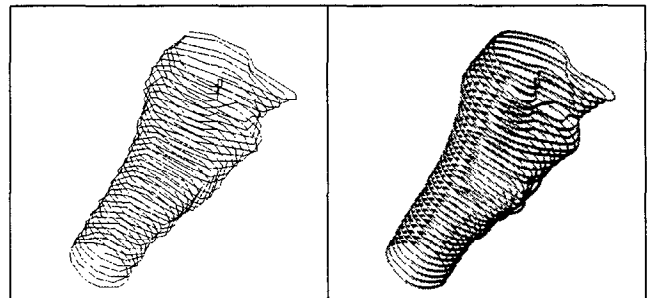


Figure 5.5: The figure on the left shows a stack of input polygonal contours of a human femur. The right shows the  $G^1 D_4$ -regular curves interpolating the vertices of the contours.

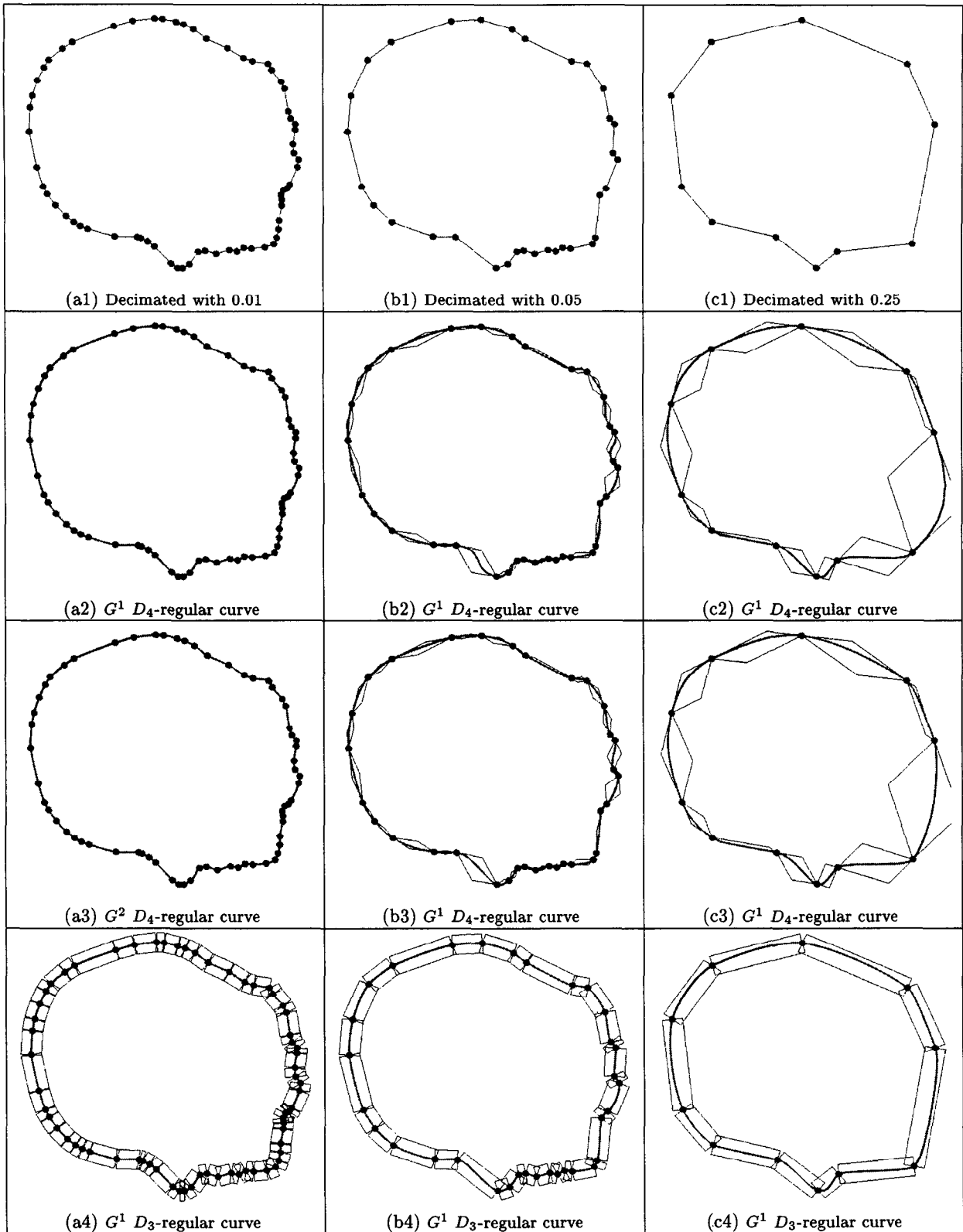


Figure 5.6: The figures in the first row show the multiresolution representation of the input data. The geometry errors are chosen to be 0.01, 0.05 and 0.25, respectively. The second row is the corresponding  $G^1 D_4$ -regular curves with a parallelogram chain. The third row is the corresponding  $G^2 D_4$ -regular curves with a parallelogram chain. The last row is the corresponding  $G^1 D_3$ -regular curves with a rectangle chain, where the width of the rectangles are chosen to be 0.3.

## 6 Conclusions and Future Work

We have characterized the lowest bi-degree of tensor BB-form polynomial to achieve  $G^1$  and  $G^2$  continuous regular algebraic spline curves. Using the lowest bi-degree, we constructed explicit spline curve families whose members satisfied given  $G^1$  and  $G^2$  interpolation conditions. We also derived a geometric interpretation of each spline curve family, so that the shape of the individual curves can be controlled intuitively.

Finally, we point that the  $D_3$  and  $D_4$ -regular curves used in this paper can be extended to 3D space curves. The parallelogram and the rectangle become the parallelepiped (see Fig 6.1(a)) and the cubocoid (see Fig 6.1(b)) volume cells, respectively. The  $G^1$  and  $G^2$  regular space spline curve segments are now defined by the intersection of two zero contours of trivariate tensor product polynomial functions in BB-form within each volume cell. Properties and data fitting schemes for these implicitly defined space curves are currently being researched.

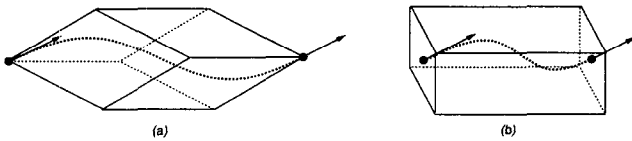


Figure 6.1: Implicitly spline curve segment defined within (a) parallelepiped and (b) cubocoid, using dual trivariate tensor product polynomial functions in BB-form.

## References

- [1] C. Bajaj, J. Chen, R. J. Holt, and A. N. Netravali. Energy formulations of A-splines. *Computer Aided Geometric Design*, 15(5):1-21, 1998.
- [2] C. Bajaj and G. Xu. A-Splines: Local Interpolation and Approximation using  $C^k$ -Continuous Piecewise Real Algebraic Curves. Accepted for publication in. *Computer Aided Geometric Design*, 1999.
- [3] V. Bhaskaran, B. Natarajan, and Konstantinos Konstantinides. Optimal piecewise-linear compression of images. In M. Cohn J. Storer, editor, *Proc. of 1993 Data Compression Conference*, pages 168 - 177. IEEE Computer Society Press, 1993.
- [4] G. Farin. *Curves and Surfaces for Computer Aided Geometric Design: A Practical Guide, Second Edition*. Academic Press Inc., 1990.
- [5] Michael Kass, Andrew Witkin, and Demetri Terzopoulos. Snakes: Active Contour Models. *International Journal of Computer Vision*, pages 321-331, 1988.
- [6] Floater M. On zero curves of bivariate polynomials. *Advances in Comp. Mathematics*, 1996.
- [7] S. Osher and J. A. Sethian. Fronts Propagating with Curvature-Dependent Speed: Algorithms Based on Hamilton-Jacobi Formulation. *Journal of Computational Physics*, 79:12-49, 1988.
- [8] M. Paluszny and R. R. Patterson. A family of tangent continuous algebraic splines. *ACM Transaction on Graphics*, 12,3:209-232, 1993.
- [9] M. Paluszny and R. R. Patterson. Geometric control of  $G^2$ -cubic A-splines. *Computer Aided Geometric Design*, 13,3:261-287, 1998.
- [10] R. Patterson. Parametric Cubics as Algebraic Curves. *Computer Aided Geometric Design*, 5:139-159, 1988.

- [11] J. Peters. Evaluation of Multivariate Bernstein-Bézier on a regularly partitioned simplex. *ACM Transaction on Graphics*, to appear.
- [12] T. Sederberg, J. Zhao, and A. Zundel. Approximate parametrization of algebraic curves. In W. Strasser and H-P. Seidel, editors, *Theory and Practice of Geometric Modeling*, pages 33-54. Springer Verlag, 1988.
- [13] T.W. Sederberg. Planar piecewise algebraic curves. *Computer Aided Geometric Design*, 1(3):241-255, 1984.
- [14] J. A. Sethian. *Level Set Methods*. Cambridge University Press, 1996.
- [15] G. Taubin, F. Cukierman, S. Sullivan, J. Ponce, and D. Kriegman. Parameterized Families of Polynomials for Bounded Algebraic Curve and Surface Fitting. *IEEE Transactions on Pattern Analysis and Machine Intelligence*, 16(3):287-303, 1994.
- [16] G. Xu, C. Bajaj, and Xue W. Regular Algebraic Curve Segments(I)-Definition and Properties. Technical Report, ICM-95-21, Institute of Computational Mathematics, 1995. To appear in CAGD.